Shahid Chamran University of Ahvaz

Irrigation Sciences and Engineering (JISE)
Vol. 48, No. 4, Winter 2026, p. 1-17

Journal homepage: https://jise.scu.ac.ir

Research Paper

Experimental Study of Longitudinal Extension Effects on Scour Patterns Around Single and Grouped Piers

Farinaz Erfani Fard[1], Seyed Amin Asghari Pari[2*] and Lotfollah Emadali[3]

1- *Department of Civil Engineering, Behbahan Khatam Alanbia University of Technology, Behbahan, Iran*
2*- *Corresponding Author, Associate Professor, Department of Civil Engineering, Behbahan Khatam Alanbia University of Technology, Behbahan, Iran (asghari_amin@bkatu.ac.ir)*
3- *Assistant Professor, Department of Civil Engineering, Behbahan Khatam Alanbia University of Technology, Behbahan, Iran.*

ARTICLE INFO

Artlcle history:
Received: 15 February 2025
Revised: 10 May 2025
Accepted: 18 May 2025
Available online: 04 January 2026

Keywords:
Local scour, Square pier, Maximum scour depth, Single pier, pier group.

TO CITE THIS ARTICLE:

Erfani Fard, F., Asghari Pari, S. A., Emadali, L. 2026. 'Experimental Study of Longitudinal Extension Effects on Scour Patterns Around Single and Grouped Piers', *Irrigation Sciences and Engineering*, 48(4), pp. 1-17. doi: 10.22055/jise.2025.49041.2155

Abstract

Scour, defined as the erosion of a streambed around obstructions, poses significant risks to bridge piers, leading to structural failures and causing economic and human losses. This study investigates the effects of pier shape (modified by adding triangular and rounded noses to rectangular piers) and longitudinal extension on scour depth around single piers and pier groups. Experiments were conducted on rectangular single piers with a fixed width of 0.03 meters and varying lengths (length-to-width ratios, L/D = 1–9), as well as on groups of three-square piers with a side length of 0.03 meters and varying center-to-center distances (S/D = 2–5). The results demonstrate that adding a nose significantly reduces scour depth. The triangular nose on a rectangular pier (L/D = 9) achieved the highest reduction, decreasing the maximum scour depth by 80% compared to the benchmark model. In pier group configurations, increasing the distance between piers generally led to greater scour depths, as each pier began to act independently. The maximum scour depth observed in the S/D = 3 model increased by 25% relative to the benchmark. As pier spacing increased, scour holes became more distinct. Additionally, equipping the first pier in a group with a nose effectively diverted flow away from the piers, reducing scour more effectively than in nose-less configurations, with the triangular nose proving most effective. Overall, pier groups exhibited significantly higher scour depths than single piers.

Introduction

Local scour around bridge piers, resulting from complex interactions between hydrodynamic forces and sediment transport, remains a critical challenge in hydraulic engineering. This phenomenon is primarily driven by three key mechanisms: (1) the formation of a horseshoe vortex at the pier's upstream face, (2) the downward flow that accelerates sediment entrainment, and (3) the wake vortices propagating downstream, which further erode the riverbed (Ahmed, 1995; Dey and Raikar, 2007; Wang et al., 2017). Given its potential to compromise bridge stability, extensive research has characterized scour dynamics, with emphasis on the influence of flow conditions, sediment properties, and pier geometry (Melville and Raudkivi, 1977; Breusers et al., 1977; Dey and Raikar, 1995; Pandey et al., 2020; Vijayasree and Eldho, 2021). Recent experimental and numerical advancements have deepened insights into scour processes. Guan et al. (2019), for instance, demonstrated that the horseshoe vortex system evolves from a single vortex to a complex multi-vortex structure during scour development. Their findings revealed that the primary vortex intensifies in strength and size

as the scour hole deepens, highlighting the dynamic nature of flow-pier interactions. To mitigate scour risks, countermeasures such as collars (Farooq et al., 2023; Heidarpour et al., 2010), slots (Moncada et al., 2009), and optimized pier geometries have been explored (added for parallel structure). Streamlined shapes (e.g., elliptical piers) reduce scour depth by up to 29.16% compared to square piers (Khan et al., 2024), while octagonal configurations disrupt vortex formation more effectively (Farooq and Grumman, 2019).

Pier dimensions and alignment relative to flow direction significantly influence scour characteristics. Experimental studies by Khan et al. (2017) demonstrated that increasing pier size from 0.03 × 0.03 m to 0.05 × 0.05 m elevates scour depth, highlighting the sensitivity of scour to structural scale. Similarly, Fenocchi and Natale (2016) used numerical and physical modeling to investigate rectangular piers of different lengths and flow attack angles. According to their results, for rectangular piers with different length-to-width ratios (L/D = 1, 1.5, 2, and 3), scour increases significantly as the flow attack angle increases. Omara et al. (2022) studied scour around rectangular piers with length ratios L/D = 1-9 in shallow flow. Their research showed that the maximum scour occurred in rectangular piers with L/D = 4.5. These findings collectively emphasize the importance of geometric considerations in pier design.

While most research focuses on single pier configurations, modern bridge designs often employ pier groups to accommodate wider spans. This necessitates a thorough understanding of the interplay between multiple piers, including vortex interference, spacing effects, and collective scour patterns. Research on tandem and side-by-side arrangements has revealed that scour depth depends critically on the dimensionless spacing ratio (S/D), where S represents the center-to-center distance between piers and D denotes the pier width. For instance, Ataie-Ashtiani and Aslani-kordkandi (2013) compared the flow patterns around a tandem circular pier group and single piers. Their results showed that the turbulent kinetic energy, turbulence intensity, and vortex strength around the piers group were lower than around single piers. They also stated that the bed shear stress between the two piers is about twice that around the piers, and the scour between them is approximately 15% greater than for the single pier case. Complementary numerical investigations by Habibi et al. (2023) identified S/D = 2 as a critical threshold for tandem pier groups, beyond which pier interactions diminish significantly. The configuration of pier groups also plays a pivotal role in scour development. A comparative study by Vijayasree and Eldho (2016) demonstrated that oblong pier arrangements reduce scour volume by 55.63% relative to twin circular piers, illustrating the benefits of aerodynamic shaping. Zhou et al. (2020) examined the influence of the angled pier arrangement and spacing in the group of three cylindrical piers. They said that when piers are placed in a line, the distance between the piers does not determine the scour depth. However, when the flow attack angle is greater than zero, depending on the attack angle, pier diameter, and pier spacing, the maximum scour depth shifts from the first pier to the second and third piers, which they attributed to a reinforcing effect. They also came up with an equation for predicting maximum scour depth based on their data and data from other experiments.

Overall, Recent research on scour patterns around bridge piers highlights key influences of pier geometry, flow conditions, and pier arrangements. Experimental studies demonstrate that rectangular piers induce the deepest scour due to intensified horseshoe vortices, whereas streamlined shapes (e.g., sharp-nosed or lenticular) minimize scour depth (Baranwal et al., 2023; Al-Jubouri et al., 2024). Scour depth correlates positively with flow velocity and frontal area (Baranwal et al., 2023), as well as water depth and discharge (Kadam and Dawari, 2024). For grouped piers, spacing critically affects scour dynamics: increasing the distance between side-by-side piers reduces scour depth (Movahedi et al., 2011), and in tandem arrangements, maximum

scour depth at the upstream pier occurs at a spacing of two pier diameters, with reduced scour at the downstream pier due to sheltering effects (Hassan et al., 2020). Lenticular piles consistently outperform circular and square shapes in scour mitigation (Tariq et al., 2022), and non-uniform twin piers further underscore spacing-dependent scour variations (Ravanfar et al., 2024).

The primary objective of this paper is to investigate the combined effects of two factors, pier length extension and nose shape alteration, on scour depth. This topic has received limited attention in previous studies, which typically examine either pier nose shape or pier length in isolation. In contrast, this study systematically analyzes the interaction between these two parameters and presents their simultaneous effects on scour depth and patterns. Moreover, it includes a comparative analysis of scour around square pier groups with various nose shapes (such as triangular and circular) at different distances. This innovative approach contributes to the design of more erosion-resistant bridge piers. 36 experiments were conducted on rectangular single piers of varying lengths and groups of three piers at different spacings, with configurations including no nose, triangular noses, and round noses under consistent laboratory conditions.

Experimental Setup

The experiments for this study were conducted in a flume with glass walls, 0.6 meters in width and height, and 6 meters in straight length at the Hydraulics Research Laboratory of Behbahan Khatam Alanbia University of Technology. At the flume inlet, two perpendicular metal mesh screens and a Styrofoam piece installed on the water surface were used to minimize fluctuations caused by water pumping. A gate was installed at the flume outlet to adjust the water level. The maximum flow rate of the current was 90 liters per second, measured by an ultrasonic flowmeter with an accuracy of ± 0.01. The flowmeter's sensors were positioned on the outlet pipe from the pump, just before entering the flume. The sediment particles used were non-cohesive sedimentary particles with a specific gravity of ρ_s = 2650 kg/m³ and a median diameter of d_{50} = 0.0012 m. All experiments were performed under constant conditions: clear water, a discharge of 25.7 liters per second, the average approach velocity, u, was 0.285 m/s, and the velocity ratio, u/u_c = 0.96. The water depth was maintained 0.15 meters above the sediment surface. This study used rectangular single piers with a constant width of 0.03 meters, varying lengths (length-to-width ratios L/D = 1, 2, 3, 4, 5, 6, 7, 9), and a height of 0.45 meters. Three square piers, each measuring 0.03 meters in both length and width, were utilized in the pier group experiments. The center-to-center distance between piers in the pier groups, experiments was chosen as 2, 3, 4, and 5 times the pier width (S/D = 2, 3, 4, 5). Additionally, to examine the effect of the nose on scour, all experiments were conducted in three conditions: rectangular cross-section (Rec), with a triangular nose (Tria), and with a round nose (Round). In this study, the L/D =1, Rec test is adopted as the benchmark model. An Acoustic Doppler Velocimeter (ADV) was used to investigate flow development. Due to the instrument's operational constraints—requiring full submersion of its probes—the first measurable point was 0.5 m below the water surface. Velocity profiles were plotted along the flume's centerline within the pier-installed region. As shown in Fig. (1), the velocity profiles remain uniform along the channel's longitudinal direction, with profiles at different locations overlapping. Under the current experimental conditions, the flow was fully developed along the straight section containing the bridge piers.

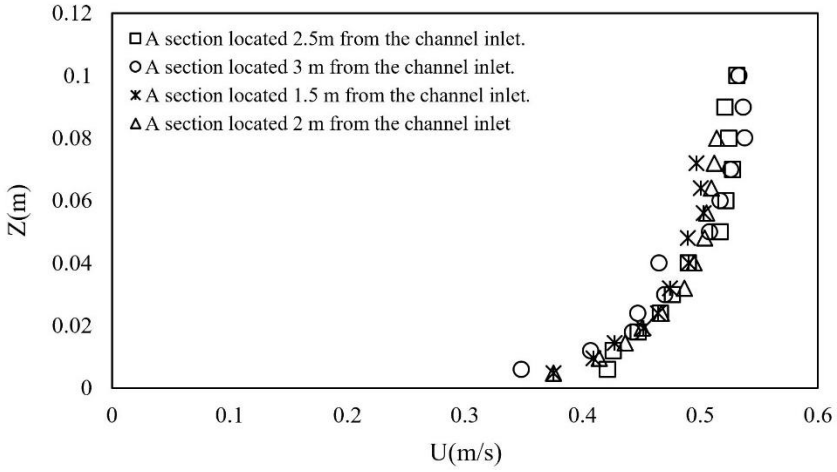


Fig. 1- Velocity profiles at various distances from the channel inlet.

In this study, Melville's equation was employed to estimate the critical flow velocity (Melville, 1997); subsequently, Kramer's mean transport criterion was applied to verify the threshold at which sediment initiation occurs. According to the Kramer sediment transport criterion, this threshold is usually characterized by the displacement of medium-sized sediment particles within the bed material (Kramer, 1935). While this method is primarily qualitative, it effectively captures the initial stages of sediment transport, providing a reliable indicator of when sediment begins to shift. Since laboratory observations were specifically conducted for the study in question, they were generally considered more reliable, and the results matched to real experimental conditions. The methodology was as follows: First, an experiment without a pier (to prevent localized scour due to the presence of a pier) was conducted to determine the critical velocity. The water depth was set (0.15 m in this study), and the flow discharge was gradually increased until, at a point in the channel and bed where the flow was fully developed and unaffected by side walls, the first bed particle was dislodged and transported downstream. Using the relation $Q = Au_c$, the average u_c was determined as the critical velocity. Subsequently, experiments were conducted at a specified discharge (25.7 L/s), lower than the critical discharge, and u/u_c = 0.96 to ensure clear-water scour conditions.

Dimensional Analysis

The parameters influencing local scour around bridge piers are diverse. Extensive studies have been conducted in this regard, with Ettema et al. (1998) and Ansari et al. (2002) identifying scour depth as a function of influential parameters, including flow characteristics, channel properties, pier specifications, bed conditions, and fluid properties. The present study aims to investigate the impact of longitudinal pier development, both as single and group configurations, as well as the effect of nose placement on local scour around piers. Consequently, the parameters affecting the scour hole depth (d_s) are as follows: flow depth (y), flow velocity (u), fluid density (ρ), the kinematic viscosity of flow (ν), median sediment size (d_{50}), bed sediment density (ρ_s), bridge pier width (D), pier length (L), geometric standard deviation of bed particle distribution (σ_g), time (t), gravitational acceleration (g), the center-to-center spacing between piers (S), and nose shape parameter (β).

$$d_s = f(u, \rho, \nu, d_{50}, \rho_s, D, L, \sigma_g, t, g, S, \beta,) = 0 \quad (1)$$

For dimensional analysis in this study, the Buckingham π theorem was employed. Based on this method, 11 dimensionless parameters were formed. The flow depth for this study was

selected based on criteria established by Breusers et al. (1977), Ettema (1980), and Raudkivi (1986), which indicate that when $y/D > 3$ to 4, the maximum scour depth becomes independent of flow depth. According to Xie (2011) and Fael et al. (2016), the equilibrium scour depth does not depend on sediment coarseness for $D/d_{50} \geq 25$–50. Additionally, Lee and Sturm (2009) demonstrated that the maximum relative pier scour depth occurs at $b/d_{50} \approx 25$. To eliminate the channel wall effect on scour depth, $B/D \geq 10$ should be maintained (Melville and Chiew, 1999). The discharge rate, duration, flow depth, and median sediment size remain constant in all experiments. Finally, the dimensional analysis of parameters affecting scour depth is obtained as follows:

$$\frac{d_s}{D} = f(\frac{L}{D}, \frac{S}{D}, \beta) \quad (2)$$

Test Conditions

After preparing the bed, the pump was activated, and the gate installed downstream was adjusted to achieve a height of 0.15 meters above the bed. To prevent initial scour caused by the flow, water entry into the flume began with a low discharge, and then, after establishing the necessary flow depth, the discharge was gradually increased to reach the intended 25.7 liters per second. Once the flow reached the desired conditions, the scour experiment commenced, marking the initial time. In previous studies (Melville and Chiew, 1999; Sheppard et al., 2014; Lança et al., 2013), various criteria were stated for equilibrium scour depth under steady flow. According to Kumar et al. (1999), equilibrium time is defined as the point when the scour rate is equal to or less than one millimeter over 3 hours. Mia and Mago (2003) halted their experiments when the rate of scour advancement became less than 1 mm/hr. Moncada et al. (2009) selected a criterion where the changes in scour depth over 2 hours are less than 1 mm to define the onset of the equilibrium state. To achieve equilibrium in the scouring experiments of the present research, the equilibrium time for all experiments was considered to be approximately 72 hours. In this study, the equilibrium depth was defined as a depth at which, in the last 8 hours of each test, the changes in the depth of the hole are equal to or less than 1 mm. Fig.(2)demonstrates that scour depth progression around the benchmark model stabilized over time, with marginal fluctuations, confirming the establishment of equilibrium conditions in the experiment. At the end of the experiment, the water supply system was turned off, and the water level adjustment gate was lowered to allow for gentle drainage. After the complete drainage of water, a bed profiler device was employed to measure topographic changes caused by bed scouring. This device consists of a mobile, intelligent carriage equipped with a laser with a measurement error of ±1 mm. Fig.(3)shows the setup before starting tests, and Fig.(4)shows a selected test.

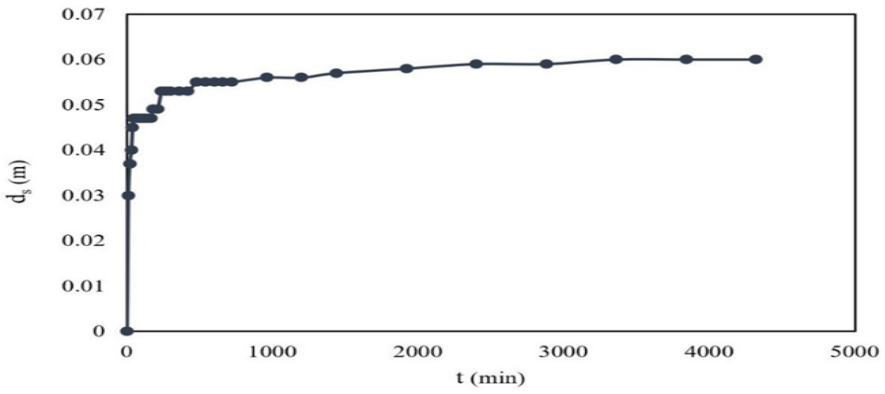


Fig. 2- Equilibrium Scour Depth Progression: Benchmark Model test

 DOI: 10.22055/jise.2025.49041.2155



Fig. 3- Setup and Calibration of Experimental Apparatus for Laboratory Testing: a) Smoothing of bed sediment, b) placement of the pier in the bed sediment, c) leveling of the pier.

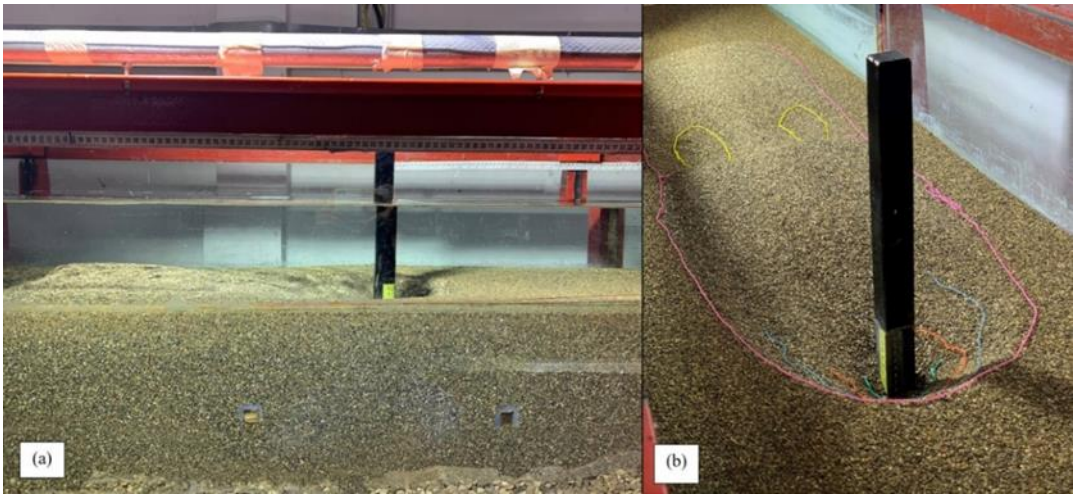


Fig. 4- L/D = 1, Rec Test: a) In-Progress Testing, b) Scouring Completed.

Results and Discussion

Flow Pattern

The presence of a bridge pier in the river cross-section leads to the formation of complex turbulent structures around the pier. This study examined changes in surface flow paths by analyzing wood chip movements on the water surface. Small wood chips were sprinkled on the surface, revealing flow patterns as they passed near piers. To illustrate the changes in the surface flow path caused by the bridge piers, wood chips were first sprinkled on the water. Then, a video was recorded from above. The recorded video was converted into sequential images, which were then analyzed using the PIVLab code in MATLAB software. Fig. (5)and Fig. (6)show the output images from PIVLab.

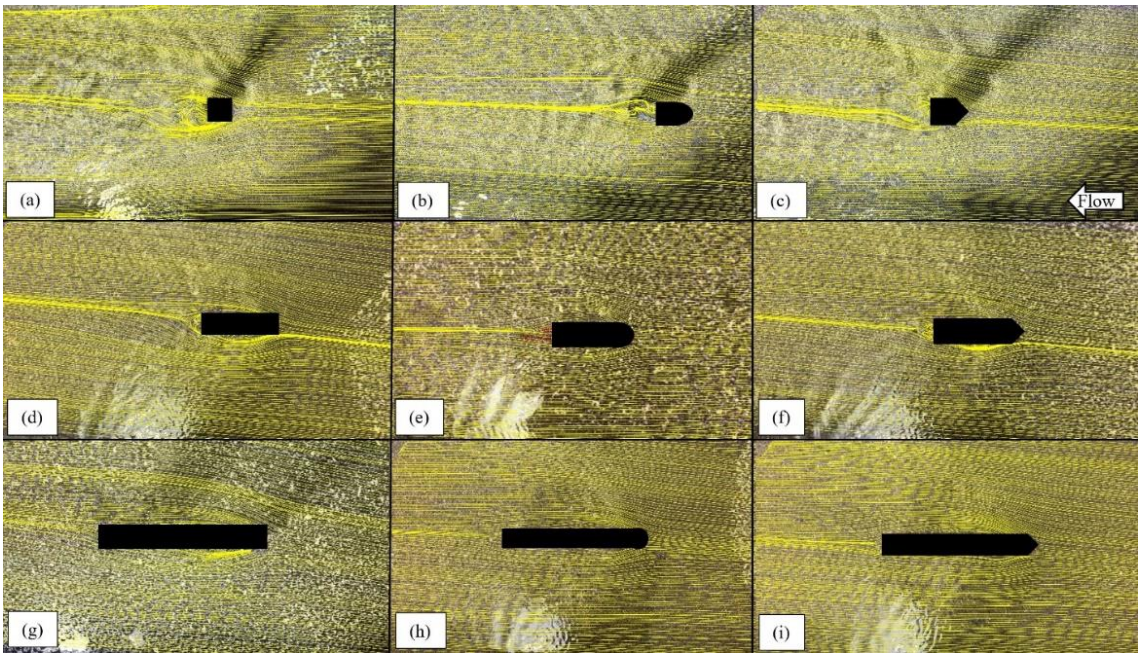


Fig. 5- Surface flow conditions around single pier: a) L/D = 1, Rec, b) L/D = 1, Round, c) L/D = 1, Tria, d) L/D = 4, Rec, e) L/D = 4, Round, f) L/D = 4, Tria, g) L/D = 9, Rec, h) L/D = 9, Round, and i) L/D = 9, Tria.

As shown in Fig. (5a), when the flow impacts a single pier with an *L/D* ratio of 1, it symmetrically deflects around the pier, forming two downstream vortices. As the pier length increases, the surface flow mechanism changes, reducing the size of the surface vortices and consequently decreasing the oscillations downstream of the pier. For an extended single pier with an L/D ratio of 9, the flow, after striking the pier, is deflected to the sides and continues along and beyond the pier without noticeable oscillation. The addition of a nose to the single pier, which alters the surface area impacted by the flow, results in smaller vortices forming behind the pier and a reduction in oscillations over a shorter downstream distance. In extended single piers, the combination of elongation and the presence of a nose causes the flow, after striking the nose, to be diverted and then to continue along a straight path without oscillation beside the pier. As illustrated in Fig. (6), in experiments involving a group of piers, the upstream pier initially deflects the flow to the sides, allowing it to enter the space between the two piers. This interaction leads to the formation of surface oscillations and vortices behind each pier. When the spacing between piers increases, the flow first impacts the upstream pier, then deflects to the side, and subsequently flows between the two piers. In this case, the larger spacing increases both the flow area and the volume of flow passing through. As depicted in Fig. (5), this results in more pronounced surface oscillations and turbulence between the piers compared to cases with smaller pier spacing.

 DOI: 10.22055/jise.2025.49041.2155

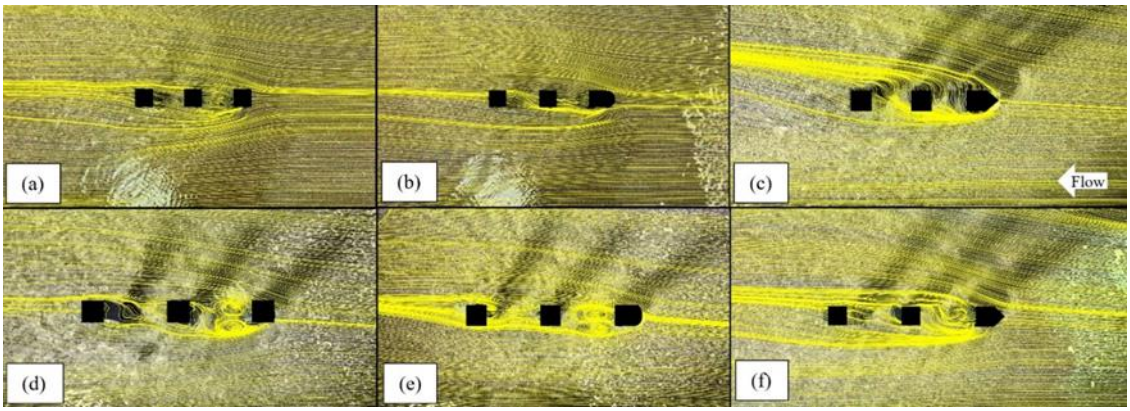


Fig. 6- Surface flow conditions around pier groups: a) *S/D* = 3, Rec, b) *S/D* =3, Round, c) *S/D* = 3, Tria, d) *S/D* = 5, Rec, e) *S/D* = 5, Round, and f) *S/D* = 5, Tria.

It was observed that adding a nose to the upstream pier in the pier group reduced surface oscillations between the two piers compared to configurations without a nose. Furthermore, the triangular nose, due to its smaller contact area with the flow, was more effective in minimizing surface oscillations between the piers than the round nose.

Scour Pattern

Comparison of the results in Fig. (7)reveals a direct correlation between pier length and scour depth reduction. The *L/D* = 9, Rec model, which features the longest pier, exhibits a 35% reduction in maximum scour depth compared to the benchmark case. This decrease can be attributed to the weakened interaction of primary vortices, reducing their collective intensity. Additionally, the increased pier length promotes smoother flow passage around the structure, thereby decreasing turbulence. As a result, both vortex strength and localized scour are mitigated. The observed trend—where scour depth decreases with increasing pier length (while pier width remains constant)—is consistent with established flow dynamics and vortex behavior (Vijayasree and Eldho, 2016; Chibana et al., 2022; Tao et al., 2013; Muzzammil et al., 2004). These findings are further supported by Kharbeche (2022), Guemou et al. (2016), and Omara et al. (2022), who demonstrated that lengthening the pier while maintaining a constant width alters scour mechanisms, ultimately reducing scour depth. As illustrated in Fig. (7a) triangular nose on the upstream side of the shortest pier (*L/D* = 1, Tria) reduces the maximum scour depth by 60% compared to the benchmark model, whereas a rounded nose (*L/D* = 1, Round) achieves a 50% reduction. Notably, the triangular nose yields a 20% lower scour depth than the rounded nose for *L/D* = 1, confirming that pier shape significantly influences scour depth and flow dynamics. Consistent with prior studies (Baranwal et al., 2023; Elshahat and Elnikhely, 2023; Vijayasree et al., 2019), sharp or triangular noses outperform round and rectangular designs in scour mitigation. This improvement stems from the nose's flow-deflecting effect, which reduces pressure buildup on the pier surface. For piers with short longitudinal extensions, the triangular nose promotes lateral flow deflection, isolating the horseshoe vortex from downstream vortices and weakening vortex intensity. In contrast, rectangular piers with flat faces exhibit the deepest scour due to unmitigated vortex development (Farooq and Gumman, 2019; Ismael et al., 2015; Tao et al., 2013). In this study, the triangular nose (sharp nose) also showed better results in minimizing the scour hole depth than the round nose. The simultaneous effects of nose geometry and pier length on maximum scour depth were also examined. The results indicate that both the addition of a nose and an increase in pier length significantly reduce scour depth. Specifically, the *L/D* =9, Tria

model reduced scour depth by 80%, while the *L/D* =9, Round model achieved a reduction of 68% compared to the benchmark model. These findings demonstrate a strong synergistic effect from elongating the pier and incorporating a nose. Among the models tested, the *L/D* =9, Tria model emerged as the best performer, reducing maximum scour depth by 69% compared to the *L/D* =9, Rec model, 33% compared to the *L/D* =9, Round model, and 50% compared to the *L/D* =1, Tria model.

Fig. (8)shows the bed profile changes at the end of the experiment for some single pier tests. The longitudinal extension of the pier significantly reduces both the depth of scour and the extent of erosion on the bed, while also reducing the volume of sediment mounds formed downstream Moreover, the combined effects of the pier's longitudinal extension and the design of its nose—whether triangular or round— reduce scoured area, limiting scouring to the bed adjacent to the pier

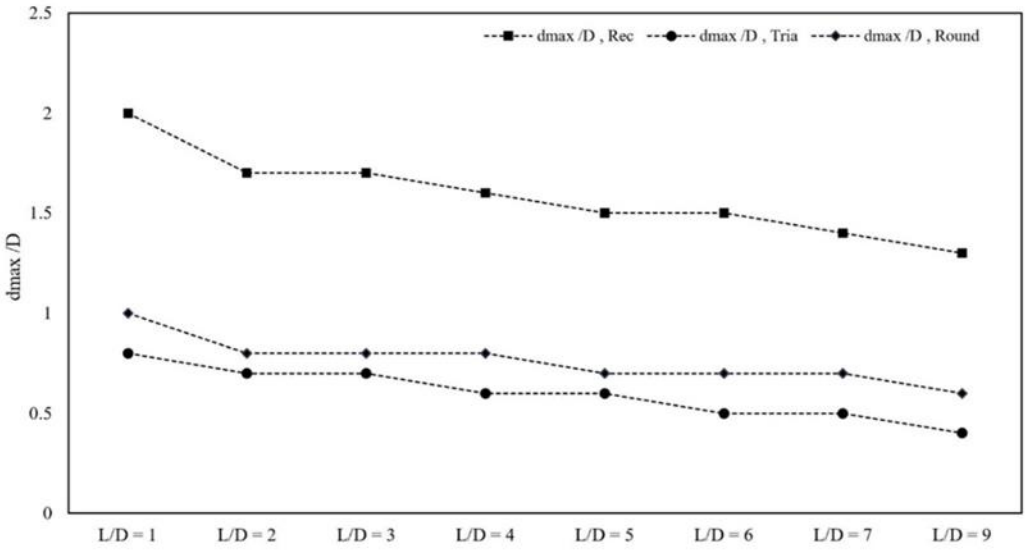


Fig. 7- The maximum scour depth in single piers

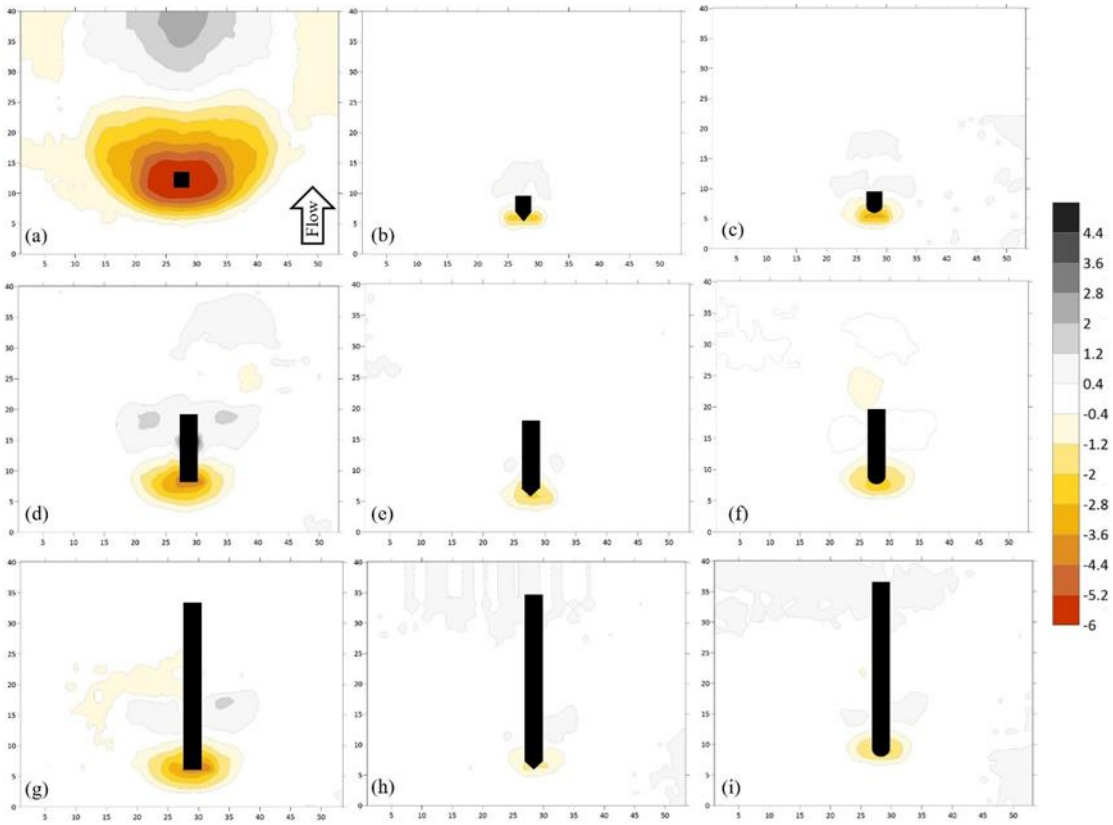


Fig. 8- Topographic status of the single pier: a) L/D = 1, Rec, b) L/D = 1, Tria, c) L/D = 1, Round, d) L/D = 4, Rec, e) L/D = 4, Tria, f) L/D = 4, Round, g) L/D = 9, Rec, h) L/D = 9, Tria, and i) L/D = 9, Round.

As illustrated in Fig. (9), in the pier group experiments without noses, the maximum scour depth occurred at the first pier, followed by the second and third piers. This pattern occurs because unobstructed flow impacts the first pier at maximum intensity, making it act as a defensive barrier for downstream piers. The shielding effect of the upstream pier reduces scour at the subsequent piers, consistent with previous findings (Salim and Jones, 1996; Ataie-Ashtiani and Beheshti, 2006; Kim et al., 2014; Hassan et al., 2020). Further analysis of Fig. (9) indicates that in nose-less tests, the maximum scour depth (observed at the first pier) increases with the spacing ratio (*S/D*) from 2 to 4, driven by interactions between the horseshoe vortex systems of adjacent piers. Specifically, increasing *S/D* from 2 to 3 elevates the scour rate by 14%, while a further increase to *S/D* = 4 results in a 9% rise compared to the *S/D* = 2 test. However, at *S/D* = 5, the vortex interaction weakens, reducing the maximum scour depth. The diminished overlap of vortices around each pier contributes to this decline. In the *S/D* = 5 Rec model, the maximum scour depth decreased by 4.5% compared to the *S/D* = 2, Rec model, though it remained 15% higher than the benchmark model. These results align with prior studies (Habibi et al. 2024; Hassan et al., 2020), reinforcing the relationship between pier spacing, vortex dynamics, and scour depth. This is evident in the topographic images of the pier group without a nose in Fig. (10), whereas the distance between the piers in the group increases, the scour holes also become separated, with each pier having its own scour hole. According to previous studies (Dargahi, 1990; Das et al., 2016) and the analysis of single piers presented in this research, the shape of the bridge pier nose significantly influences the vortex pattern and scour distribution. As illustrated in Fig. (9), in the experiments conducted on piers with noses, both the triangular and round noses resulted in the highest transfer of scour from the first pier

to the second. This phenomenon can be attributed to the effect of the nose shape on the flow impact dynamics. Based on the analysis of Fig. (9), the addition of a nose to the first pier in the group configuration significantly reduced the maximum scour depth across all piers compared to the no-nose scenario. The triangular nose design yielded substantial reductions in scour depth relative to the *S/D* = 2, Rec model: 59% (*S/D* = 2, Tria), 23% (*S/D* = 3, Tria), 64% (*S/D* = 4, Tria), and 68% (*S/D* = 5, Tria). Similarly, the rounded nose design demonstrated reductions of 50%, 27%, 23%, and 65% for *S/D* = 2, 3, 4, and 5, respectively. In addition, the maximum scour depths for pier groups with triangular and round noses at various spacing distances were compared. It was observed that in the *S/D* = 2 and *S/D* = 3 models, the round nose outperformed the triangular nose. Conversely, in the *S/D* = 4 model, the triangular nose demonstrated superior performance. At a spacing distance of *S/D* = 5, the effectiveness of both nose designs was nearly equivalent. The topographic images of pier groups with various nose designs, as illustrated in Fig.(10), indicate that the presence of a nose on the first pier minimizes the bed area exposed to scour both upstream and downstream of the piers.

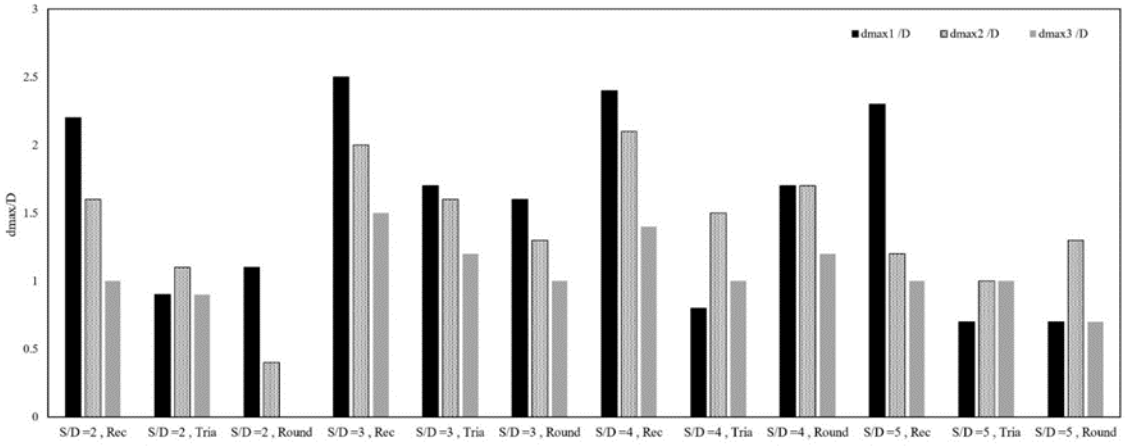


Fig. 9- The maximum scour depth in pier groups.

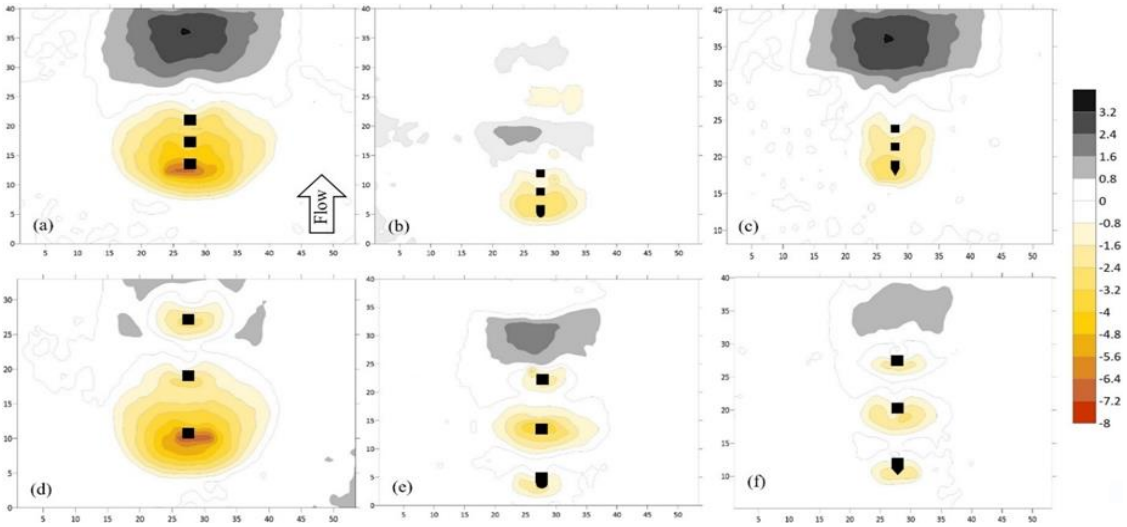


Fig. 10- Topographic status of the pier groups: a) S/D = 2, Rec, b) S/D = 2, Round, c) S/D = 2, Tria, d) S/D = 5, Rec, e) S/D = 5, Round, and f) S/D = 5, Tria.

 DOI: 10.22055/jise.2025.49041.2155

Comparing the results of the extended single pier tests with those of the corresponding pier group tests, it can be concluded that the maximum scour depth for the extended single pier is consistently less than that of the first pier in the corresponding group. This is most probably due to the interference effect of the second downstream pier in the pier group experiments. Overlapping of scour holes is observed due to the presence of a downstream pier, and as the bed level behind the upstream pier decreases, it helps transport the bed sediment eroded from the front of the first pier. As a result, the maximum scour depth at the upstream pier is higher than in the case when the flow is not constricted. It is also important to note that the upstream pier is subjected to the reinforcing effect of the downstream pier (Amini et al., 2013). Also, the topographic images reveal that the extended single piers, compared to the corresponding extended pier groups, have a smaller surface area of the sediment bed affected by scour. scour result for all experiments is shown in Table (1).

Table. 1- Scour results.

Type of piers	*L*/*D*	Pier shape	*S*/*D*	d_{max1} /*D*	d_{max2} /*D*	d_{max3}/*D*
Single pier	1	Rec	*	2	*	*
	2	Rec	*	1.7	*	*
	3	Rec	*	1.7	*	*
	4	Rec	*	1.6	*	*
	5	Rec	*	1.5	*	*
	6	Rec	*	1.5	*	*
	7	Rec	*	1.4	*	*
	9	Rec	*	1.3	*	*
	1	Tria	*	0.8	*	*
	2	Tria	*	0.7	*	*
	3	Tria	*	0.7	*	*
	4	Tria	*	0.6	*	*
	5	Tria	*	0.6	*	*
	6	Tria	*	0.5	*	*
	7	Tria	*	0.5	*	*
	9	Tria	*	0.4	*	*
	1	Round	*	1	*	*
	2	Round	*	0.8	*	*
	3	Round	*	0.8	*	*
	4	Round	*	0.8	*	*
	5	Round	*	0.7	*	*
	6	Round	*	0.7	*	*
	7	Round	*	0.7	*	*
	9	Round	*	0.6	*	*
Group pier	1	Rec	2	2.2	1.6	1
	1	Rec	3	2.5	2	1.5
	1	Rec	4	2.4	2.1	1.4
	1	Rec	5	2.3	1.2	1
	1	Tria	2	0.9	1.1	0.9
	1	Tria	3	1.7	1.6	1.2
	1	Tria	4	0.8	1.5	1
	1	Tria	5	0.7	1	1
	1	Round	2	1.1	0.4	0.0
	1	Round	3	1.6	1.3	1
	1	Round	4	1.7	1.7	1.2
	1	Round	5	0.7	1.3	0.7

Conclusion

This study investigated the effects of longitudinal pier extensions and nose shape modifications on local scour under controlled conditions. Key findings include:

Pier Elongation (No Nose): Increasing the length-to-width ratio (*L/D*) up to 9 effectively reduced scour by up to 35% by separating upstream and downstream vortex systems.

Nose Modification (*L/D* = 1): Adding a triangular or round nose reduced scour by 60% and 50%, respectively, with the triangular shape proving more effective at deflecting flow.

Combined Effects (*L/D* = 9 with Nose): A strong synergistic effect was observed—triangular and round-nosed piers reduced scour by 80% and 68%, respectively, compared to the benchmark.

Pier Groups: Upstream piers experienced the most scour; nose modifications reduced scour across all piers, with round noses performing better at close spacing (*S/D* = 2–3) and triangular noses at intermediate spacing (*S/D* = 4).

Spacing Effects: Scour increased at *S/D* = 2–4 due to vortex interference, but decreased at *S/D* = 5 as vortex interaction weakened and distinct scour holes formed.

Single vs. Group Piers: Pier groups showed deeper scour than single piers due to flow interaction between multiple piers.

These results emphasize the benefits of combining pier elongation with nose shaping to significantly reduce scour risk. Future work should focus on field validation and scaling effects.

Acknowledgment

This research has no acknowledgments.

Conflict of Interest

The authors declared no potential conflicts of interest concerning the research, authorship, and publication of this article. Confirmation.

Funding

The authors received no financial support for the research, authorship, and publication of this article.

Data Availability Statements

Data Availability Statement: All information and results are presented in the text of the article.

Authors' contribution

First Author: Farinaz Erfanifard (50%): Responsible for writing the manuscript, conducting the experiments, and analyzing the results.

Second Author: Seyed Amin Asghari Pari (Corresponding Author, 40%): Served as the thesis supervisor, controlled the overall work, and reviewed the results.

Third Author: Lotfala Emadali (10%): Provided consultation and overall review.

Notation

The following symbols are used in this paper:

A = flow cross-section
B = flume width;
D = pier width;
d_{50} *= median grain diameter;*
ds = local scour depth;
d_{maxi} *= the maximum scour depth around the ith pier;*
g = gravitational acceleration;
L = pier length;
n = number of piers;
S = center-to-center spacing between piers;
t= time;
u = flow velocity;
u_c *= critical flow velocity;*
y = flow depth;
ρ *= fluid density;*
ρ_s *= bed sediment density;*
β *= nose shape parameter;*
σ_g *= geometric standard deviation of bed particle distribution;*
ν *= kinematic viscosity of flow.*

References

1- Ahmed, F. 1995. Flow and erosion around bridge piers. Dissertation, University of Alberta.

2- Aksoy, A.O., Bombar, G., Arkis, T. and Guney, M.S., 2017. Study of the time-dependent clear water scour around circular bridge piers. *Journal of hydrology and hydromechanics*, *65*(1), p.26. DOI: 10.1515/johh-2016-0048.

3- Al-Jubouri, M., Ray, R.P. and Abbas, E.H., 2024. Prediction of scour depth for diverse pier shapes utilizing two-dimensional Hydraulic Engineering Center's River Analysis System sediment model. *Fluids*, *9*(11), p.247. doi.org/10.3390/fluids9110247.

4- Amini, A., Melville, B.W., Ali, T.M. and Ghazali, A.H., 2013. Closure to "Clear-Water Local Scour around Pile Groups in Shallow-Water Flow" by Ata Amini, Bruce W. Melville, Thamer M. Ali, and Abdul H. Ghazali. *Journal of Hydraulic Engineering*, *139*(6), pp.680-681. doi.org/10.1061/(ASCE)HY.1943-7900.00007.

5- Ansari, S.A., Kothyari, U.C. and Ranga Raju, K.G., 2002. Influence of cohesion on scour around bridge piers. *Journal of hydraulic research*, *40*(6), pp.717-729. doi.org/10.1080/00221680209499918

6- Ataie-Ashtiani, B. and Aslani-Kordkandi, A., 2013. Flow field around single and tandem piers. *Flow, turbulence and combustion*, *90*, pp.471-490.

7- Ataie-Ashtiani, B. and Beheshti, A.A., 2006. Experimental investigation of clear-water local scour at pile groups. *Journal of Hydraulic Engineering*, *132*(10), pp.1100-1104. doi.org/10.1061/(ASCE)0733-9429(2006)132:10(1100)

8- Baranwal, A., Das, B.S. and Setia, B., 2023. A comparative study of scour around various shaped bridge pier. *Engineering Research Express*, *5*(1), p.015052. DOI 10.1088/2631-8695/acbfa1.

9- Breusers, H.N.C., Nicollet, G. and Shen, H.W., 1977. Local scour around cylindrical piers. *Journal of hydraulic research*, *15*(3), pp.211-252. doi.org/10.1080/00221687709499645

10- Das, S., Das, R. and Mazumdar, A., 2016. Comparison of local scour characteristics around two eccentric piers of different shapes. *Arabian Journal for Science and Engineering*, *41*, pp.1199-1213.

11- Dargahi, B., 1990. Controlling mechanism of local scouring. *Journal of hydraulic engineering*, *116*(10), pp.1197-1214. doi.org/10.1061/(ASCE)0733-9429(1990)116:10(119.

12- Dey, S. and Raikar, R.V., 2007. Characteristics of horseshoe vortex in developing scour holes at piers. *Journal of Hydraulic Engineering*, *133*(4), pp.399-413. doi.org/10.1061/(ASCE)0733-9429(2007)133:4(399).

13- Dey, S., Bose, S.K. and Sastry, G.L., 1995. Clear water scour at circular piers: a model. *Journal of Hydraulic Engineering*, *121*(12), pp.869-876. doi.org/10.1061/(ASCE)0733-9429(1995)121:12(869.

14- Chibana, T., Quiocho, R. and Watanabe, K., 2022. Role of grain size distribution and pier aspect ratio in scouring and sorting around bridge piers. *Water*, *14*(13), p.2066. doi.org/10.3390/w14132066.

15- Elshahat, E. and Elnikhely, E., 2023. Influence of the Shape and Properties of the Bridge Pier's Nose on Scour Depth. *The Egyptian International Journal of Engineering Sciences and Technology*, *42*(1), pp.15-22. Doi: 10.21608/EIJEST.2022.150217.1167.

16- Ettema, R., Melville, B.W. and Barkdoll, B., 1998. Scale effect in pier-scour experiments. *Journal of Hydraulic Engineering*, *124*(6), pp.639-642. doi.org/10.1061/(ASCE)0733-9429(1998)124:6(639).

17- Ettema, R. 1980. Scour at bridge piers, Report No. 216, University of Auckland, New Zealand.

18- Fael, C., Lança, R. and Cardoso, A., 2016. Effect of pier shape and pier alignment on the equilibrium scour depth at single piers. *International Journal of Sediment Research*, *31*(3), pp.244-250. doi.org/10.1016/j.ijsrc.2016.04.001.

19- Farooq, R. and Ghumman, A.R., 2019. Impact assessment of pier shape and modifications on scouring around bridge pier. *Water*, *11*(9), p.1761. doi.org/10.3390/w11091761.

20- Farooq, R., Azimi, A.H., Tariq, M.A.U.R. and Ahmed, A., 2023. Effects of hooked-collar on the local scour around a lenticular bridge pier. *International Journal of Sediment Research*, *38*(1), pp.1-11. doi.org/10.1016/j.ijsrc.2022.07.002.

21- Fenocchi, A. and Natale, L., 2016. Using numerical and physical modeling to evaluate total scour at bridge piers. *Journal of Hydraulic Engineering*, *142*(3), p.06015021. doi.org/10.1061/(ASCE)HY.1943-7900.0001096.

22- Guan, D., Chiew, Y.M., Wei, M. and Hsieh, S.C., 2019. Characterization of horseshoe vortex in a developing scour hole at a cylindrical bridge pier. *International journal of sediment research*, *34*(2), pp.118-124. doi.org/10.1016/j.ijsrc.2018.07.001.

23- Guemou, B., Seddini, A. and Ghenim, A.N., 2016. Numerical investigations of the round-nosed bridge pier length effects on the bed shear stress. *Progress in Computational Fluid Dynamics, An International Journal*, *16*(5), pp.313-321. doi.org/10.1504/PCFD.2016.078753.

24- Habibi, K., Fard, F.E. and Pari, S.A.A., 2023. Investigation of the flow field around bridge piers on a non-eroding bed using FLOW-3D. In *22nd Iranian Conference on Hydraulics*.

25- Habibi, K., Fard, F.E., Pari, S.A.A. and Shafai-Bejestan, M., 2024. Experimental and theoretical study of sediment scour around angled bridge piers. *Canadian Journal of Civil Engineering*, *51*(10), pp.1091-1108. doi.org/10.1139/cjce-2023-0277.

26- Hassan, Z.F., Karim, I.R. and Al-Shukur, A.H.K., 2020. Effect of interaction between bridge piers on local scouring in cohesive soils. *Civil Engineering Journal*, *6*(4), pp.659-669. DOI: 10.28991/cej-2020-03091498.

27- Heidarpour, M., Afzalimehr, H. and Izadinia, E., 2010. Reduction of local scour around bridge pier groups using collars. *International Journal of Sediment Research*, *25*(4), pp.411-422. doi.org/10.1016/S1001-6279(11)60008-5.

28- Ismael, A., Gunal, M. and Hussein, H., 2015. Effect of bridge pier position on scour reduction according to flow direction. *Arabian Journal for Science and Engineering*, *40*, pp.1579-1590.

29- Kadam, G. and Dawari, B., 2024. Experimental, analytical, and numerical evaluation of Bridge Pier scouring. *Civ Environ Eng*, *20*(1), pp.411-425. DOI: 10.2478/cee-2024-0032.

30- Khan, M., Tufail, M., Ajmal, M., Haq, Z.U. and Kim, T.W., 2017. Experimental analysis of the scour pattern modeling of scour depth around bridge piers. *Arabian Journal for Science and Engineering*, *42*, pp.4111-4130.

31- Khan, K.A., Waseem, M. and Alam, M., 2024. Experimental investigation of pier scour depth and its scour hole pattern for different shapes. *Journal of Infrastructure, Policy and Development*, *8*(4), p.3096.

32- Kharbeche, M., 2022. *The Role of Pier Shape and Aspect Ratio on Local Scour with and Without Sacrificial Piles* (Master's thesis, University of Windsor (Canada)).

33- Kim, H.S., Nabi, M., Kimura, I. and Shimizu, Y., 2014. Numerical investigation of local scour at two adjacent cylinders. *Advances in water resources*, *70*, pp.131-147. doi.org/10.1016/j.advwatres.2014.04.018.

34- Kramer, H., 1935. Sand mixtures and sand movement in fluvial model. *Transactions of the American Society of Civil Engineers*, *100*(1), pp.798-838. doi.org/10.1061/TACEAT.000465.

35- Kumar, V., Raju, K.G.R. and Vittal, N., 1999. Reduction of local scour around bridge piers using slots and collars. *Journal of hydraulic engineering*, *125*(12), pp.1302-1305. doi.org/10.1061/(ASCE)0733-9429(1999)125:12(1302).

36- Lança, R., Fael, C., Maia, R., Pêgo, J.P. and Cardoso, A.H., 2013. Clear-water scour at pile groups. *Journal of Hydraulic Engineering*, *139*(10), pp.1089-1098. doi.org/10.1061/(ASCE)HY.1943-7900.0000770.

37- Lee, S.O. and Sturm, T.W., 2009. Effect of sediment size scaling on physical modeling of bridge pier scour. *Journal of hydraulic engineering*, *135*(10), pp.793-802. doi.org/10.1061/(ASCE)HY.1943-7900.0000091.

38- Melville, B.W. and Chiew, Y.M., 1999. Time scale for local scour at bridge piers. *Journal of Hydraulic Engineering*, *125*(1), pp.59-65. doi.org/10.1061/(ASCE)0733-9429(1999)125:1(59).

39- Melville, B.W., 1997. Pier and abutment scour: integrated approach. *Journal of hydraulic Engineering*, *123*(2), pp.125-136. doi.org/10.1061/(ASCE)0733-9429(1997)123:2(125).

40- Melville, B.W. and Raudkivi, A.J., 1977. Flow characteristics in local scour at bridge piers. *Journal of Hydraulic Research*, *15*(4), pp.373-380. doi.org/10.1080/00221687709499641

41- Mia, M.F. and Nago, H., 2003. Design method of time-dependent local scour at circular bridge pier. *Journal of Hydraulic Engineering*, *129*(6), pp.420-427. doi.org/10.1061/(ASCE)0733-9429(2003)129:6(420).

42- Moncada-M, A.T., Aguirre-Pe, J., Bolivar, J.C. and Flores, E.J., 2009. Scour protection of circular bridge piers with collars and slots. *Journal of Hydraulic Research*, *47*(1), pp.119-126. doi.org/10.3826/jhr.2009.3244

43- Movahedi, N., Dehghani, A.A., Aarabi, M.J. and Zahiri, A.R., 2011. Temporal evolution of local scour depth around side-by-side piers. *Journal homepage: http://www. ojceu. ir/main*, *82*, p.86.

44- Muzzammil, M., Gangadharaiah, T. and Gupta, A.K., 2004, June. An experimental investigation of a horseshoe vortex induced by a bridge pier. In *Proceedings of the institution of civil engineers-water management* (Vol. 157, No. 2, pp. 109-119). Thomas Telford Ltd. doi.org/10.1680/wama.2004.157.2.109.

45- Omara, H., Ookawara, S., Nassar, K.A., Masria, A. and Tawfik, A., 2022. Assessing local scour at rectangular bridge piers. *Ocean Engineering*, *266*, p.112912. doi.org/10.1016/j.oceaneng.2022.112912.

46- Pandey, M., Azamathulla, H.M., Chaudhuri, S., Pu, J.H. and Pourshahbaz, H., 2020. Reduction of time-dependent scour around piers using collars. *Ocean Engineering*, *213*, p.107692. doi.org/10.1016/j.oceaneng.2020.107692.

47- Raudkivi, A.J., 1986. Functional trends of scour at bridge piers. *Journal of hydraulic engineering*, *112*(1), pp.1-13. doi.org/10.1061/(ASCE)0733-9429(1986)112:1(1).

48- Ravanfar, S.M., Mohammadpour, R. and Sabzevari, T., 2024. Experimental study of local scour around non-uniform twin piers. *International Journal of River Basin Management*, *22*(3), pp.429-444. doi.org/10.1080/15715124.2023.2167823

49- Salim, M. and Jones, J.S., 1996. Scour around exposed pile foundations. In *North American water and environment congress & destructive water* (pp. 2202-2211). ASCE.

50- Sheppard, D.M., Melville, B. and Demir, H., 2014. Evaluation of existing equations for local scour at bridge piers. *Journal of Hydraulic Engineering*, *140*(1), pp.14-23. doi.org/10.1061/(ASCE)HY.1943-7900.0000800.

51- Tao, J., Gao, Q. and Yu, X., 2013. *Assessment of the Effects of Pier Configurations on the Flow Pattern and Scour: A CFD Modeling Approach* (No. 13-2840).

52- Tariq, M., Khan, A. and Khan, M., 2022. Experimental study of scour hole depth around bridge pile using efficient cross-section. *Applied Sciences*, *12*(10), p.5205. doi.org/10.3390/app12105205.

53- Vijayasree, B. and Eldho, T., 2016. Experimental study of scour around bridge piers of different arrangements with same aspect ratio.

54- Vijayasree, B.A., Eldho, T.I., Mazumder, B.S. and Ahmad, N., 2019. Influence of bridge pier shape on flow field and scour geometry. *International Journal of River Basin Management*, *17*(1), pp.109-129. doi.org/10.1080/15715124.2017.1394315

55- Vijayasree, B.A. and Eldho, T.I., 2021. A modification to the Indian practice of scour depth prediction around bridge piers. *Current Science*, *120*(12), pp.1875-1881.

56- Wang, C., Yu, X. and Liang, F., 2017. A review of bridge scour: mechanism, estimation, monitoring and countermeasures. *Natural Hazards*, *87*, pp.1881-1906.

57- Xie, Z., 2011. *Theoretical and numerical research on sediment transport in pressurized flow conditions*. The University of Nebraska-Lincoln.

58- Zhou, K., Duan, J.G. and Bombardelli, F.A., 2020. Experimental and theoretical study of local scour around three-pier group. *Journal of Hydraulic Engineering*, *146*(10), p.04020069. doi.org/10.1061/(ASCE)HY.1943-7900.0001794.

© 2026 The Author(s). Published by Shahid Chamran University of Ahvaz. This is an open-access article distributed under the terms of the Creative Commons Attribution License (http://creativecommons.org/licenses/by/4.0), which permits unrestricted use, distribution, and reproduction in any medium, provided the original work is properly cited.